JACOBS PUBLISHERS

OPEN ACCESS

Clinical Journal of Ophthalmology

Research Article

Oxydative Metabolism in Optic Nerve Myelin: New Perspectives in Hereditary Optic Neuropathies

Silvia Ravera[1], Martina Bartolucci[1], Paola Ramoino[2], Daniela Calzia[1], Carlo Traverso[3], Isabella Panfoli[1]*

[1]*DIFAR-Laboratorio di Biochimica, Università di Genova, Viale Benedetto XV/3, 16132, Genova, Italy.*

[2]*DISTAV, Università di Genova, Corso Europa 30, 16132 Genova, Italy.*

[3]*Clinica Oculistica, DINOGMI, Università di Genova, Viale Benedetto XV, 1 16132 Genova,Italy.*

**Corresponding author:* *Isabella Panfoli, University of Genova, School of Medical and Pharmaceutical Sciences, DIFAR-Biochemistry Lab. 16132 GENOVA, Tel: + 39 010 353 7397, Fax + 39 010 353 8153, Email: Isabella.Panfoli@unige.it*

Received: 07-16-2014
Accepted: 08-20-2014
Published: 08-23-2014

Abstract

Myelin from both central and peripheral nervous system was shown to express functional FoF1-ATP synthase and respiratory chain complexes that conduct an aerobic metabolism, to supportthe axonal energy demand. Along this view, it has been proposed that the trophic action of myelin that has been recognized to cause degeneration of chronically demyelinated is a major and not replaceable energetic role. Optic nerve displays great metabolic demand. Its demyelisation is implicated in Leber's hereditary optic neuropathy (LHON), one of the most frequent hereditary optic neuropathies caused by mutations in respiratory Complex I. The specific damage of retinal ganglion cells (RGC) in LHON has not been clarified yet.

In this work, by biochemical analyses, we show that myelin isolated from bovine optic nerve, conducts an extra-mitochondrial oxidative phosphorylation, displaying active respiratory complexes I to IV, as well as oxygen consumption and ATP synthesis activity, sensitive to specific inhibitors. Immunohystochemical microscopy shows that myelin basic protein and respiratory complex I colocalize in optic nerve sections.

Data support the notion that mutations of Complex I would impair oxidative phosphorylation, not only in neuronal mitochondria, but also in myelin of the optic nerve. This may shed new light on some optic neuropathies.

Keywords: brain metabolism; demyelinating disease; extramitochondrial oxidativephosphorylation; glia; LHON; nerve degeneration; optic neuritis.

Abbreviation:

ANT - Adenosine Nucleotide Translocase;
BSA - Bovine Serum Albumin;
CLSM - Confocal Laser Scanning Microscopy;
CNS - Central Nervous System;
EGTA - Ethylene Glycol Tetraacetic Acid;
ETC - Electron Transport Chain;
GA - Glutaraldehyde; Ide, Idebenone;
IM - Isolated Myelin;
MBP - Myelin Basic Protein;
LHON - LeberHereditary Optic Neuropathy;
MW - MolecularWeight;
NS - Nervous System;
OXPHOS - Oxidative Phosphorylation;
PBS - Phosphate BufferedSaline;
PNS - Peripheral Nervous System;
RGC - Retinal Ganglion Cells;
R.O.D. - Relative OpticalDensity;
ROS - Reactive Oxygen Species;
TEM - Transmission Electron Microscopy;
TIM - Mitochondrial Import Inner Membrane Translocase;
WB - Western Blot;

Introduction

An oxidative metabolism was shown to occur in both peripheral and central myelin [1–4], independent of mitochondria. Both CNS and PNS myelin may be a site of aerobic chemical energy supply for axons, together with the axonal mitochondria. A role for connexons in the transfer ofATP to the axoplasm was suggested [5]. Moreover, the aerobic ATP production by myelin wasimpaired [4] in a model of dys/demyelinating disease (CMT1A) in spite of a normal functioning of Schwann cell mitochondria. An apparently pervasive ectopic OXPHOS expression has been Reviewed [6].

CNS and retina critically depend on oxygen supply [7] and are sensitive to "mitochondrialdysfunction" [8,9]. Mitochondria have been implicated in several neurodegenerative diseases [10]accompanied by loss of myelin. The glia appears essential in maintaining optimal CNS function [11]and the proliferation of oligodendrocytes and astrocytes is responsive to trophic cues associatedwith neuronal activity [12]. Loss of myelin in demyelinating diseases does not simply cause a loweringof speed of conduction but also an axonal degeneration [13]due to a lack of trophic support [14] andenergy depletion [15,16]. A demyelization is observed also in Leber hereditary optic neuropathy (LHON), a maternally inherited optic atrophy due to mitochondrial dysfunction. LHON initially affects the parvocellular Retinal Ganglion Cells (RGC) (papillomacular bundle), causingdyschromatopsia, loss of visual acuity, cecocentralscotomas and temporal optic atrophy [17]. Three primary pathogenic mitochondrial DNA (mtDNA) mutations affecting the mitochondrial respiratoryComplex I (NADH dehydrogenase) were shown to be causative of LHON [18]. 95% of individuals with LHON have one of three point mutations of mtDNA: m.11778G>A (MT-ND4), by far the mostcommon among Caucasian populations; m.14484T>C (MT-ND6), or m.3460G>A (MT-ND1)[8]. Theseverity of the biochemical phenotype is higher for the 3460/ND1 and the 11778/ND4 mutations [19] that have been linked to insufficient energy supply in the mitochondria of the optic nerve neurons [20]. However, the ultimate reason why LHON targets RGC has not yet been clarified. Mitochondrialdisorders are a group of human diseases characterized by defects of the mitochondrial machinery for oxidative phosphorylation (OXPHOS), primarily affecting visual system and the Central and Peripheral Nervous System (CNS and PNS) [21,22]. Manifestations of these diseases, apart from opticnerve degeneration, include ataxia, dementia, and deafness [23].

In this paper, we focused on myelin purified from optic nerve to assess whether it plays an energetic role for the retinal ganglion cells (RGC) axons. Isolated Myelin (IM) from bovine optic nerve was assayed for respiratory and ATP synthetic properties by biochemical and confocal microscopy techniques. Overall data are consistent with the idea of optic nerve myelin conducting oxidative phosphorylation, and suggest that Complex I dysfunction in myelin like in LHON mutations may cause an ATP depletion and imbalance between the energy demand and supply to RGC axon negatively influencing its survival by a retrograde degeneration.

Materials and Methods

Myelin Isolation

Myelin was isolated from 3 g of cattle optic nerve, obtained from a local slaughterhouse bythe 'floating up' sucrose gradient modification of the method by Norton and Poduslo [24], asdescribed [1–4]. The method involves steps of centrifugation at 75000 g for 30 min of to isolate a layer of crude myelin from the homogenate, and two steps of hypotonic shock in 10 volumes of ultrapure water plus subsequent centrifugation to isolate purified myelin. Nerves were homogenized in 20 vol. (w/v) 0.32 M sucrose in 2 mM EGTA. Protease inhibitor cocktail (Sigma-Aldrich) 30 μg/ml 5-Fluorouracil and 20μg/ml Ampicillin were present throughout isolation while CyclosporinA [25] was absent. Centrifugation was conducted in a Beckman FW-27 rotor (Beckman, Fullerton, CA, USA).

TEM microscopy

IM and optic nerves were fixed in 2% paraformaldehyde plus 0.2% glutaraldehyde (GA), included in gelatin and freezed in liquid nitrogen. Ultrathin sections (60 nm thick) were obtainedwith a microtome and put onto classical copper grids [1].

Electrophoresis, Semiquantitive Western Blot (WB) and Quantification

Denaturing electrophoresis (SDS-PAGE) was performed using a Laemmli [26]protocol. Antibodies used were: rabbit polyclonal Ab against beta subunit of ATP synthase (Sgma-Aldrich), diluted 1:5000 in Phosphate Buffered Saline (PBS); mouse monoclonal anti-MBP, that identifies an18-20 kDa band (); Anti-Na+/K+ ATPase (AbCam, Cambridge, UK , Anti-alpha 1 ,ab7671) and anti-Adenosine Nucleotide Translocase (ANT) (Santa Cruz, CA, USA), diluted 1:400 in PBS; anti– Mitochondrial import inner membrane translocase (TIM), subunit 8A (Santa Cruz, CA, USA), diluted 1:200 in PBS. Secondary Abswas from Sigma-Aldrich. Protein Molecular Weight (MW) markers were from BioRad (BioRad, CA, USA). Quantitative densitometry was performed using ChemiDoc (BioRad, CA, USA). Results wereexpressed as Relative Optical Density (R.O.D.).

Detection of mitochondria DNA in IM

A primer pair, to specifically detect bovine mitochon-

drial DNA, was designed by the on-line Primer3 software program. The sequences for primers were: forward, 5'-GCTAAGACCCAAACTGGGATT-3'; reverse, 5'-AGCCCATTTCT-TCCCATTTC-3'. Amplification reactions were carried out in a total volume of 20 ml, and reaction mixtures containing 5x PCR-Buffer, 2 mM MgCl2, 1 pmol of each primer, 0.2 mMdeoxynucleosidetriphosphates, and 1 U of Ampli-Taq DNA polymerase (PerkinElmer, Emeryville, CA, USA). Mitochondria enriched fraction and IM vesicles were subjected to a PCR program consisting of 1 cycle at 95 °C for 2 min, 30 cycles at: 95 °C for 30 s for denaturing, 56 °C for 45 s for annealing,and 72 °C for 30 s for extension, and 1 cycle at 72 °C for 7 min [3].

Oxygraphic measurements

O2 consumption was assayed in homogenates, crude myelin and IM from optic nerves by athermostatically controlled amperometricoxygraph (Unisense – Micro-respiration, Unisense A/S, Denmark) and a mixing device. Samples were incubated at 23°C in the following solution: 120 mMKCl, 2 mM MgCl2, 1 mM KH2PO4, 50 mMTris-HCl, pH 7.4 and 25 µg/ml ampicillin (final volume 1.7 ml) [1,3,4]. To observe the uncoupled respiration rates, 30 µM Nigericin was added before the addition of respiring substrates and inhibitors of O2 consumption: 0.7 mM NADH, 20 mMsuccinate, 40 µM rotenone and 50 µM antimycin A. To observe the ADP stimulated respiration rates, 0.045 mM ADP was added after NADH and Succinate. Mitochondria enriched-fractions were used as positive controls. In this case NADH was substituted for by 5 mM Pyruvate and 2.5 mM Malate. Respiratory rates are expressed in µM O2/min/mg. Other respiring substrates wereutilzed,i.e.: pyruvate + malate, β-hydroxybutirate, fumarate, α-ketoglutarate, glucose and galactose, all used at the concentration of 5 mM.

Assay of Redox Complexes

The four mitochondrial Complexes were assayed spectrophotometrically, according toRavera et al [1].

ATP Synthase assay.

ATP synthetic rates were measured by the luciferin/luciferase chemiluminescent method (Roche Applied Science), according to Ravera et al. [2].

Immunohistochemistry on optical nerve

Bovine optic nerves were fixed in 4% paraformaldehyde in phosphate-buffered saline (PBS, pH 7.4) for 12 h. After careful rinses in PBS, the specimen was dehydrated and embedded in Paraplast. Transversal Paraplast sections (5 µm thick) were cut and rehydrated in a decreasing ethanol series and washed in PBS (0.1 M, pH 7.4). Double-immunohistochemical stainingtechniques were carried out. Briefly, dewaxed serial sections were incubated overnight in a moist chamber at 4°C with rabbit policlonalAb against ND1 subunit of Complex I (1:100, AbCam Cambridge UK), diluted with 0.1% bovine serum albumin (BSA) in PBS then, after several washings in PBS, sections were incubated with Alexa-488-conjugated anti-rabbit antiserum (1:800; Molecular Probes, USA), for 1 hour. Then sections were incubated overnight with a mouse monoclonal Ab against MBP (1:100, AbCam Cambridge UK), and a secondary Alexa-633 conjugated anti-mouse Ab (1:800; Sigma-Aldrich). Sections were finally mounted in a glycerol/PBS (1:1) solution and examined under an inverted Leica TCS SP5 AOBS confocal laser scanning microscope, equipped with a Leica 63XPL APO NA 1.40 oil immersion objective (LeicaMicrosystems CMS, Mannheim, Germany) [1,4].

Other procedures

Mitochondria-enriched fraction from Bovine liver was obtained according to Ravera et al [27].Protein concentration was determined by Bradford method, using BSA as standard [28].

Results

Myelin characterization

Figure 1 shows the characterization of the samples deriving from the optic nerve (homogenates, crude myelin fractions, purified myelin fractions), as well as of liver mitochondria-enriched fractions, used as a control. Panel A shows the IM morphology, as observed by TEM. Sample appears to be composed by multilamellar vesicles, while other organelle seems absent. Panel B reports the spectrophotometric analysis, performed with NanoDrop (Thermo Scientific), of amplified mitochondrial DNA from mitochondria enriched fractions and IM. The dark line representing the sample extracted from mitochondria, displays a maximum of absorbance at 260 nm. By contrast, the sample extracted from IM (light line) does not dispaly an absorbance maximum, confirming that IM are not contaminated from mitochondria.

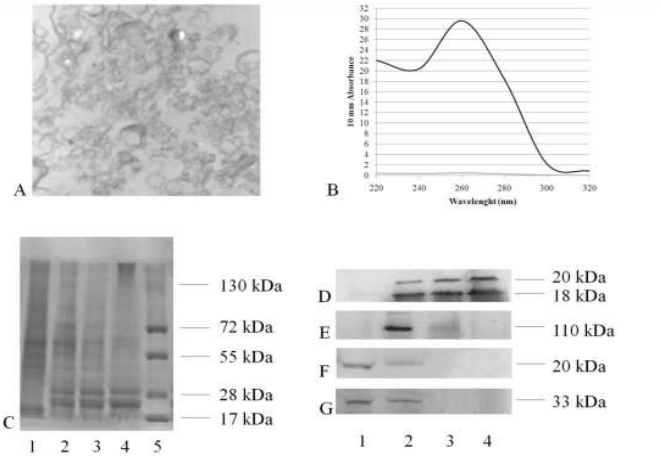

	Mitochondria enriched fraction (lane 1)	Optic Nerve Homogenate (lane 2)	Crude Myelin (lane 3)	Isolated Myelin (lane 4)
MBP (20 kDa)	0	7.2 ± 0.5	9,4 ± 1.0	14.1 ± 1.9
MBP (18 kDa)	0	11.3 ± 1.6	15.8 ± 2.0	21.4 ± 2.1
Na^+/K^+ ATPase	0	12.6 ± 0.7	2.3 ± 0.3	0
TIM	4.8 ± 0.6	2.8 ± 0.5	0	0
H ANT	4.4 ± 0.5	3.5 ± 0.3	0	0

Figure 1: Optic Nerve-derived samples characterization.
Panel A is a TEM image of the IM. Length of the membrane profiles ranges around 2 μm. Panel is representative of 10 different fields. Panel B is representative of NanoDrop® analysis of total DNA present in IM (light grey line) and in mitochondria (black line). Only the mitochondrial DNA shows an absorbance maximum at 260 nm, showing the high quality of the extracted DNA. The absorbance of the DNA contained in IM appears devoid of any evident absorbance maximum. Panel C shows the protein pattern of samples (lane 1, mitochondria-enriched fraction; lane 2, optic nerve homogenate; lane 3, crude myelin fraction; lane 4, IM; lane 5, molecular weight markers), stained with Blue Silver. Panels D, E, F, and G show the Semiquantitative Western Blot of MBP,

Na+/K+ ATPase, TIM and ANT respectively. Panel H shows the densitometric analysis of Western Blot signals, done with ChemiDoc software (BioRad). The values of densitometric analysis are expressed as Relative Optical density (ROD) ± ST DV.

Panels C-H reports the WB analysis results. Panel C shows the protein pattern as stained with Colloidal Blue Coomassie. Samples are: lane 1, mitochondria enriched fraction; lane 2, homogenate of optic nerve; lane 3, crude myelin; lane 4, IM; lane 5, MW markers. Panel D shows the chemiluminescent WB signal of MBP. Bands whose intensity increased in parallel to the isolation grade of myelin fractions are only detectable in optic nerve-derived samples. Panel E shows thatNa+/K+-ATPase was present in optic nerve homogenate, less in crude myelin and absent in IM,indicating a good isolation of IM, according to Norton and Poduslo [24]. We have utilized and Abagainst α1 subunit, as the α subunits of Na+/K+-ATPase were shown to play major roles in the NS, while the β subunits would be more important in the peripheral NS. It has been reported that fiveisoforms of Na+/K+ ATPase are expressed in nonspecific regions, Schwann cells (myelin), and thenode of Ranvier in Rat Sciatic Nerves [29].

In order to evaluate the extent of mitochondrial contamination in the purified IM, a Semiquantitative WB was carried out with Ab against ANT and TIM, two typical mitochondrial inner membrane proteins. Chemiluminescent signals of these proteins were detectable in mitochondrial enriched fraction and optic nerve homogenates (Panels F and G, respectively). WB data were confirmed by densitometric analysis (Panel H) performed with ChemiDoc (BioRad, CA, USA).

Oxygen consumption rates in IM

To verify the physiological implications of our data, we conducted an analysis of respiratory fluxes in optic nerve IM. Fig 2, Panel A reports a typical tracing of nigericin-uncoupled oxygen (O2) consumption rates. O2 consumption rates was elicited by NADH flowing in the Complex I +III + IV pathway, sensitive to inhibition by rotenone and by succinate (Complex II + III + IV) inhibited by antimycin A. To demonstrate that IM can conduct OXPHOS using several unconventional substrates, the O2 consumption was measured after the addition of: NADH,pyruvate + malate, β-hydroxybutirate, fumarate, α-ketoglutarate, glucose and galactose. Figure 2, Panel B shows that all substrates induce an O2 consumption in IM. The maximal activity wasobtained with galactose, suggesting that this substrate may play an important role in myelinmetabolism. It was reported that that in brain galactose derivatives are 50% higher than in liver [30]and that galactose enhances the oxidative phosphorylation [31]. Moreover, unlike mitochondria, IM utilize directly NADH as a respiring substrate, indicating that the respiration in IM is not due to a mitochondrial contamination.

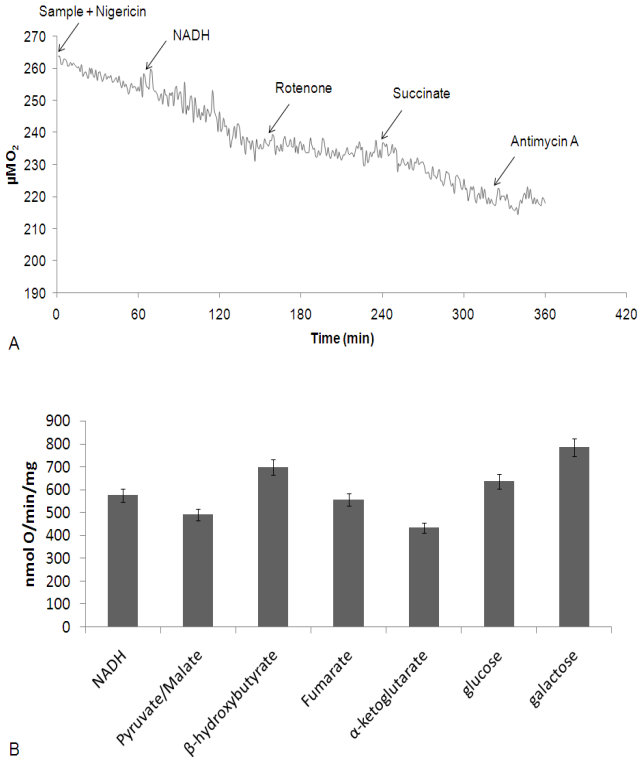

Figure 2: Respiratory rates in optic nerve IM.
Panel A reports a typical amperometric recording of Nigericin-uncoupled respiration rates elicited by the addition of NADH and Succinate as respiring substrates. These were sensitive to inhibition by rotenone and Antimycin A, respectively. Figure is representative of at least five identical experiments. Panel B shows the oxygen consumption in IM after the addition of several respiring substrates. The data are expressed as nmol O consumed/min/mg of total protein.

Complex I Assay in optic nerve IM and semiquantitative WB analysis

Figure 3, Panel A shows the semiquantitative WB analysis with Ab against ND1 subunit of Complex I. Densitometry showed that the signal in IM lane is similar to that in optic nerve homogenates (not shown). Complex I activity was assayed in mitochondria enriched-fraction (used as positive control) and in all the optic nerve-derived fractions, in the presence or absence of rotenone (Panel B). Similar results were obtained assaying the activity of the other respiratory complexes (Table 1).

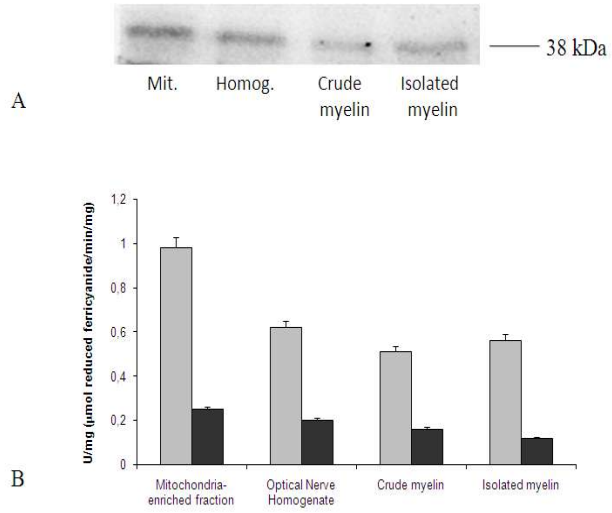

Figure 3: Complex I Assays
Panel A, semiquantitative WB analysis of Complex I (NADH-Ubiquinone oxidoreductase, subunit ND1. Samples are: Lane 1, mitochondria-enriched fraction; lane 2, optic nerve homogenate; lane 3, crude myelin fraction; lane 4, IM fraction. Panel B reports a comparison of the activity of the redox Complex I in optic nerve derived samples and in mitochondria-enriched fractions. The black columns show the activity in the presence of Rotenone, the specific inhibitors.

Table1: RespiratoryComplexesActivity

	Complex II (mU/min/mg)	Complex III (mU/min/mg)		Complex IV (mU/min/mg)	
	Sample	Sample	Sample + Antimycin A	Sample	Sample + KCN
Mitochondria	16 ± 1,9	110 ± 12	35 ± 4	76 ± 8	0
Opticnervehomog.	9,4 ± 1,1	78 ± 8	23 ± 3	40 ± 4	0
Crude myelin	6,3 ± 0,7	62 ± 7	18 ± 2	37 ± 4	0
Isolatedmyelin	6,7 ± 0,8	60 ± 7	17 ± 2	36 ± 4	0

The table reports the activity of respiratory complexes II, III and IV in the absence or presence of specific inhibitors (Antimycin A for Complex III and KCN for Complex IV). The sample used are: mitochondria enriched fraction, used as positive control, optic nerve homogenate, crude myelin and isolated myelin. The activities are expressed as mU/min/mg and reported as the mean ± S.D. Each value is representative of at least ten experiments.

ATP synthesis in optic nerve IM and WB analysis

Figure 4, Panel A shows that ATP synthase β subunit is expressed in the optic nerve IM, as assessed by WB analysis. Panel B shows the time course of ATP synthase activity, linear for the first 2 min. A maximal activity of 28 ± 3 nmol/ min/mg of protein were detected in the presence of 0.35 mM NADH, 20 mM succinate and 0.1 mM ADP. Panel C shows that IM ATP synthase wassensitive to specific inhibitors: oligomycin, inhibitor of the mitochondrial H+-pump (82 %inhibition); DCCD, inhibitor of H+-conduction (85 % inhibition); FCCP, oxidative phosphorylation uncoupler (89 % inhibition); KCN complex IV inhibitor, (96 % inhibition) and Antimycin, complex III inhibitor (66 % inhibition).

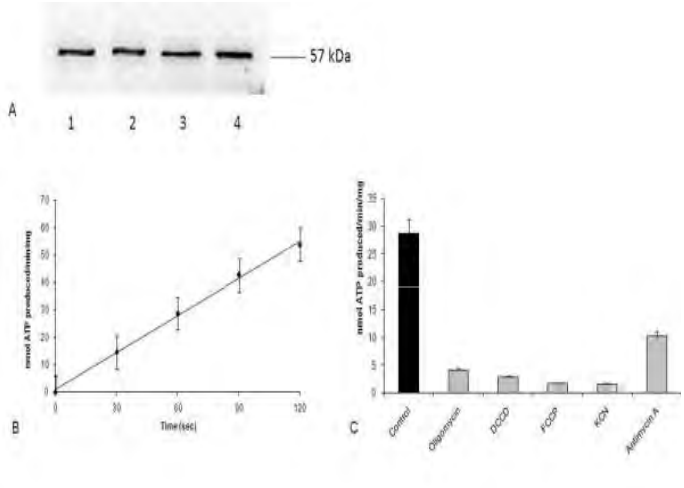

Figure 4: ATP synthesis in IM and semiquantitative WB analysis.
Panel A shows the WB signal of ATP synthase β subunit in optic nerve-derived samples (lane 2, optic nerve homogenate; lane 3, crude myelin fraction; lane 4, IM and Mitochondria (lane 1), used as positive control. Panel B shows the time course of ATP synthase activity in IM. The same assay in the absence/presence of inhibitors is in Panel C, namely Olygomycin (0.002 mM); DCCD (1 mM); FCCP (1 mM); KCN (2 mM) and antimycinA (0.02 mM).

Colocalization of MBP and ND1 on optic nerve sections

Figure 5 shows the immunofluorescence confocal laser scanning imaging of a transversal section of optic nerve stained with an Ab against ND1 (Panel A) and against MBP (Panel B). Proteins are stained by indirect fluorescence being secondary Ab for ND1 conjugated to Alexa-488 (green) and secondary Ab for MBP conjugated to Alexa-633 (red). Panel C is a merge of the fluorescence in Panels A and B.

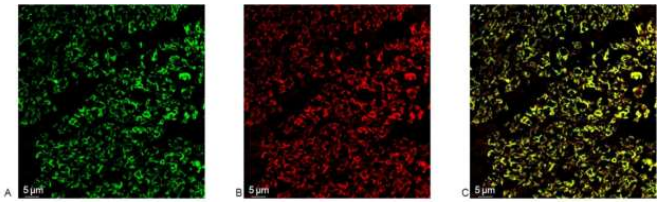

Figure 5: Confocal immunofluorescence analysis of bovine optic nerve.
Panels report the confocal laser scanning image of transversal sections of bovine optic nerve immunohystochemically stained with Ab against ND1 (Panel A) and MBP (Panel B). Proteins are stained by indirect fluorescence being secondary Ab for ND1 conjugated to Alexa-488 (green) and secondary Ab for MBP conjugated to Alexa-633 (red), respectively. Panel C is the merge of fluorescence of panels A and B.

Discussion

A major challenge in neuroscience is the identification of the main source of ATP in thenervous system that can justify its high O2 and glucose consumption [32]. It was suggested that part ofthe energy may be supplied by the glia, essential in maintaining optimal brain function [16,33]. Myelin sheath, the multilayered membrane produced by oligodendrocytes in the CNS and Schwann Cells in the PNS, plays a pivotal role in the axon surroundings [34]. The past decade has refocused the research on the relationship between axon and myelin sheath: growing evidence suggests that myelin plays aneuro-trophic role [35,36]. Myelin degeneration results in increased axonal energy demand36 and axonaldegeneration follows energy depletion [37].

The present biochemical and imaging data show that myelin isolated from the bovine optic nerve performs OXPHOS. The optic nerve in fact consumes the greatest share of oxygen in the body. Such key metabolic processes can only occur when the physiological players are perfectly coupled, in an intact lipid environment, which rules out the possibility that these activities come from mitochondrial contamination. In fact, ANT and TIM, and mitochondrial DNA were absent in Optic nerve IM (Figure 1). To confirm that our data are not due to a mitochondrial contamination during myelin isolation, confocal immunofluorescence imaging was performed on optic nerve sections that showed a colocalization of the OXPHOS proteins with MBP in myelin (Figure 5), similarly to what reported [1,2,4]. The ATP produced inside the myelin spires would sustain the highaxonal energy demand, being transported to the axoplasm through connexons [5]. Other Authors havedemonstrated that connexins are excellent ATP transporters [38].

The functionality of the Complexes I to IV in optic nerve IM, subtends the fact that also invivo the ETC could build up a proton gradient in myelin, driving ATP synthesis. Even thoughHarris and Attwell have cast doubt on the presence of a proton gradient in myelin sheath [39], ourprevious data showed that the IM possess a proton gradient [1] and that MitoTracker stains tubularstructures resembling the axons with their sheath in bovine optic nerve sections [1]. We have proposed that the OXPHOS would be process acting with a net phase separation: the proton flow wouldfollow an intra-membrane pathway, while the ATP synthesis occurs in the aqueous phase [40]. This isconsistent with previous data [41]. The recent structural data on the electron transfer Complex I [42], III [43],and ATP synthase [44] show the absence of proton channels in these proteins. We have hypothesized that protons (H+) would not be exchanged from aqueous sources to membrane sinks, but stay boundto the heads of the phospholipids, excellent proton accumulators [40]. In fact H+ spread much quickerthan foreseen by the laws of diffusion [45]. Moreover, ordered water molecules on the surface of abiological membranes are a potential barrier for H+ to diffuse [46]. On the basis of these and otherevidences [45], we have hypothesized that H+ reside in the Helmholtz layer of the membrane, beingexchanged by the ETC at the centre of the membrane thanks to cardiolipin [40,47]. The existence of an intra-membrane potential rules out the need for closed compartments in which to accumulate protons, a model that would be valid for both mitochondrial and extra-mitochondrial respiring membranes.

Besides being confirmative of the idea that both peripheral and central myelin metabolically support axons, the present data may shed new light on LHON, that is caused by mutations affectingsome subunits of mitochondrial Complex I [48], a primary reactive oxygen species (ROS) producer [49]. In fact, redox stress, such as light exposure and smoking have been postulated as causative agents. Undoubtedly, oxidative stress must be invoked in the LHON pathogenesis, as the mutated ComplexI increases its ROS production [50,51].

Loss of central vision in LHON [52-54] is attributed to progressive death of RGC. However, the exact mechanisms translating the mitochondrial dysfunction due to LHON mutations into the selective death of RGCs remains to be elucidated. Many pathogenetic mechanisms have been proposed, among which mitochondrial network dynamics, and DNA maintenance. LHON affectedindividuals only suffer from visual loss [53]. A selective RGC loss simply due to the mitochondrial disturbances remains puzzling, as the mitochondria of the other cell types bearing the same mutations, throughout the body do not exert a toxic effect on these cells. Conceivably, an inner mitochondrial membrane damaged by ROS does not represent a critical situation, as mitochondriadisplay an elevated turnover [55]. By, contrast, myelin would be prone to suffer from dysfunction of a mutated Complex I that increase the ROS burden in its lipid-rich spires. This is especially true when myelination is completed, i.e. at 20 year's age for man, when myelin turnover is slower. Even though a loss of axons is yet to be proved to initiate RGC death, it is tempting to presume that progressive

ROS accumulation would cause slowing down the ATP production, until the axoplasm becomes critically impaired. Along this vision, RGC loss would be a retrograde damage starting from axonal suffering. The idea appears consistent with the beneficial effect of treatment with an analogue of Ubiquinone (idebenone, Ide) on RGC, recently shown to promote recovery of visualacuity [8].

CONCLUSION

The present work extends our previous data on CNS [1–3] and PNS myelin [4] to the optic nerve, which consumes the greatest share of oxygen in the body. A mitochondria-independent OXPHOS in myelin isolated from optic nerves, similarly to what we had reported for bovine central and rat peripheral myelin, would stand in for the idea that myelin metabolically supports the axons of the optic nerve. This would also be supported by several proteomic studies, reviewed in Panfoli et al. [6,56]

ACKNOWLEDGEMENTS

We are indebted to Valerio Carelli (University of Bologna) and his co-workers for their invaluable contribution. The Authors have no conflict of interest to declare.

REFERENCES

1. Ravera S, Panfoli I, Calzia D, Aluigi MG, Bianchini P, et al. Evidence for aerobic ATP synthesis in isolated myelin vesicles. Int J Biochem Cell Biol. 2009; 41: 1581–1591.

2. Ravera S, Panfoli I, Aluigi MG, Calzia D, Morelli A. Characterization of Myelin Sheath F(o)F(1)-ATP synthase and its regulation by IF(1). Cell BiochemBiophys. 2011; 59: 63–70.

3. Ravera S, Bartolucci M, Calzia D, Aluigi MG, Ramoino P, et al. Tricarboxylic acid cycle-sustained oxidative phosphorylation in isolated myelin vesicles. Biochimie.2013; 95: 1991–1998.

4. Ravera S, Nobbio L, Visigalli D, Bartolucci M, Calzia D, et al. Oxydative phosphorylation in sciatic nerve myelin and its impairment in a model of dysmyelinating peripheral neuropathy. J Neurochem.2013; 126: 82–92.

5. Adriano, E., Perasso, L., Panfoli, I., Ravera, S., Gandolfo, C., et al. A novel hypothesis about mechanisms affecting conduction velocity of central myelinated fibers.Neurochem Res. 2011; 36: 1732–1739.

6. Panfoli, I., Ravera, S., Bruschi, M., Candiano, G., Morelli, A. et al. Proteomics unravels the exportability of mitochondrial respiratory chains. Expert Rev Proteomics 2011;8:231–239.

7. Kann O, Kovacs R. Mitochondria and neuronal activity. Am J Physiol Cell Physiol. 2007;292:C641–C657.

8. Sadun AA, La Morgia C, Carelli V. Leber's Hereditary Optic Neuropathy. Curr Treat Options Neurol. 2011;13:109–117.

9. Carelli V, La Morgia C, Iommarini L, Carroccia R, Mattiazzi M, et al. Mitochondrial optic neuropathies: how two genomes may kill the same cell type? Biosci Rep. 2007;27:173–184.

10. Orth M, Schapira AH. Mitochondria and degenerative disorders.Am J Med Genet.2001;106:27–36.

11. Korf J, Gramsbergen JB. Timing of potential and metabolic brain energy.J Neurochem.2007;103:1697–1708.

12. Kelic S, Levy S, Suarez C, Weinstein DE. CD81 regulates neuron-induced astrocyte cell-cycle exit. Mol Cell Neurosci.2001;17:551–560.

13. Ferguson B, Matyszak MK, Esiri MM, Perry VH. Axonal damage in acute multiple sclerosis lesions.Brain. 1997;120 (Pt 3):393–399.

14. Nave KA, Trapp BD. Axon-glial signaling and the glial support of axon function. Annu Rev Neurosci.2008; 31: 535–561.

15. Dutta R, Trapp BD. Mechanisms of neuronal dysfunction and degeneration in multiple sclerosis. ProgNeurobiol.2011;93:1–12.

16. Morelli A, Ravera S, Panfoli I. Hypothesis of an Energetic Function for Myelin. Cell BiochemBiophys 2011.

17. Carelli V, La Morgia C, Sadun AA. Mitochondrial dysfunction in optic neuropathies: animal models and therapeutic options. CurrOpin Neurol. 2013;26:52–58.

18. Mackey DA, Oostra RJ, Rosenberg T, Nikoskelainen E, Bronte-Stewart J, et al. Primary pathogenic mtDNA mutations in multigeneration pedigrees with Leber hereditary optic neuropathy. Am J Hum Genet.1996;59:481–485.

19. Pello R, Martín MA, Carelli V, Nijtmans LG, Achilli A, et al. Mitochondrial DNA background modulates the assembly kinetics of OXPHOS complexes in a cellular model of mitochondrial disease. Hum Mol Genet.2008;17:4001–4011.

20. Carelli V, Ross-Cisneros FN, Sadun AA. Optic nerve degeneration and mitochondrial dysfunction: genetic and acquired optic neuropathies. Neurochem Int. 2002;40:573–584.

21. Dimauro S. A history of mitochondrial diseases. J Inherit Metab Dis. 2011; 34(2): 261-276.

22. Zeviani M, Di Donato S. Mitochondrial disorders. Brain.2004;127:2153–2172.

23. DiMauro S. Mitochondrial diseases.BiochimBiophysActa.

2004;1658:80–88.

24. Norton WT, Poduslo SE. Myelination in rat brain: method of myelin isolation. J Neurochem.1973;21:749–757.

25. Crompton M, Ellinger H, Costi A. Inhibition by cyclosporin A of a Ca2+-dependent pore in heart mitochondria activated by inorganic phosphate and oxidative stress. Biochem J. 1988;255:357–360.

26. Laemmli UK. Cleavage of structural proteins during the assembly of the head of bacteriophage T4.Nature.1970;227:680–685.

27. Ravera S, Calzia D, Panfoli I, Pepe IM, Morelli A. Simultaneous detection of molecular weight and activity of adenylate kinases after electrophoretic separation. Electrophoresis.2007;28:291–300.

28. Bradford MM. A rapid and sensitive method for the quantitation of microgram quantities of protein utilizing the principle of protein-dye binding.Anal Biochem.1976;72:248–254.

29. Gerbi A, Sennoune S, Pierre S, Sampol J, Raccah D, et al. Localization of Na,K-ATPase α/β Isoforms in Rat Sciatic Nerves : Effect of Diabetes and Fish Oil Treatment. J Neurochem.2002;73:719–726.

30. Roser M, Josic D, Kontou M, Mosetter K, Maurer P, et al. Metabolism of galactose in the brain and liver of rats and its conversion into glutamate and other amino acids. J Neural Transm.2009;116:131–139.

31. Aguer C, Gambarotta D, Mailloux RJ, Moffat C, Dent R, et al. Galactose enhances oxidative metabolism and reveals mitochondrial dysfunction in human primary muscle cells. PLoS One 2011;6:e28536.

32. Attwell D, Laughlin SB. An energy budget for signaling in the grey matter of the brain.J Cereb Blood Flow Metab.2001;21:1133–1145.

33. Korf J. Is brain lactate metabolized immediately after neuronal activity through the oxidative pathway? J Cereb Blood Flow Metab.2006;26:1584–1586.

34. Kursula P. The current status of structural studies on proteins of the myelin sheath (Review).Int J Mol Med. 2001;8:475–479.

35. Hertz L, Peng L, Dienel GA. Energy metabolism in astrocytes: high rate of oxidative metabolism and spatiotemporal dependence on glycolysis/glycogenolysis. J Cereb Blood Flow.Metab.2007;27:219–249.

36. Trapp BD, Nave KA. Multiple sclerosis: an immune or neurodegenerative disorder? Annu Rev Neurosci.2008;31:247–269.

37. Correale J, Meli F, Ysrraelit C. [Neuronal injury in multiple sclerosis]. Med (B Aires).2006;66:472–485.

38. Goldberg GS, Moreno AP, Lampe PD. Gap junctions between cells expressing connexin 43 or 32 show inverse permselectivity to adenosine and ATP. J Biol Chem. 2002;277:36725–36730.

39. Harris JJ, Attwell D. Is myelin a mitochondrion? J Cereb Blood Flow Metab.2013;33:33–36.

40. Morelli AM, Ravera S, Calzia D, Panfoli I. Hypothesis of lipid-phase-continuity proton transfer for aerobic ATP synthesis. J Cereb Blood Flow Metab.2013;33:1838–1842.

41. Mulkidjanian AY. Proton in the well and through the desolvation barrier. BiochimBiophysActa. 2006;1757:415–427.

42. Efremov RG, Sazanov LA.Structure of the membrane domain of respiratory complex I. Nature.2011; 476:414–420.

43. Lange C, Nett JH, Trumpower BL, Hunte C. Specific roles of protein-phospholipid interactions in the yeast cytochrome bc1 complex structure. Embo J. 2001;20:6591–6600.

44. Pogoryelov D, Krah A, Langer JD, Yildiz Ö, Faraldo-Gómez JD, et al. Microscopic rotary mechanism of ion translocation in the F(o) complex of ATP synthases. Nat Chem Biol. 2010; 6:891–899.

45. Kell DB. On the functional proton current pathway of electron transport phosphorylation.An electrodic view. BiochimBiophysActa.1979;549:55–99.

46. Cherepanov DA, Junge W, Mulkidjanian AY. Proton transfer dynamics at the membrane/water interface: dependence on the fixed and mobile pH buffers, on the size and form of membrane particles, and on the interfacial potential barrier. Biophys J. 2004;86:665–680.

47. Haines TH, Dencher NA. Cardiolipin: a proton trap for oxidative phosphorylation. FEBS Lett.2002;528:35–39.

48. Rosenbluth J. A brief history of myelinated nerve fibers: one hundred and fifty years of controversy. J Neurocytol.1999;28:251–262.

49. Venditti P, Di Stefano L, Di Meo S. Mitochondrial metabolism of reactive oxygen species. Mitochondrion. 2013; 13(2):71–82.

50. Lenaz G, Baracca A, Carelli V, D'Aurelio M, Sgarbi G, et al. Bioenergetics of mitochondrial diseases associated with mtDNA mutations. BiochimBiophysActa. 2004;1658:89–94.

51. Sadun A. Acquired mitochondrial impairment as a cause of optic nerve disease. Trans Am Ophthalmol Soc. 1998;96:881–923.

52. Howell N. Leber hereditary optic neuropathy: mitochondrial mutations and degeneration of the optic nerve. Vis Res. 1997;37(24):3495–3507.

53. Man PY, Turnbull DM, Chinnery PF. Leber hereditary optic neuropathy. J Med Genet. 2002;39(3):162–169.

54. Ludtke H, Kriegbaum C, Leo-Kottler B, Wilhelm H. Pupillary light reflexes in patients with Leber's hereditary optic neuropathy. Graefes Arch ClinExpOphthalmol. 1999;237(3):207–211.

55. Gross NJ, Getz GS, Rabinowitz M. Apparent turnover of mitochondrial deoxyribonucleic acid and mitochondrial phospholipids in the tissues of the rat. J Biol Chem. 1969;244(6):1552–1562.

56. Panfoli I, Bruschi M, Santucci L, Calzia D, Ravera S, et al. Myelin proteomics: the past, the unexpected and the future. Expert Rev Proteomics. 2014; 11(3): 345–354.